

# SERS on Bimetallic Nanostructured thin films

revathy m s (✉ [revz.vijay@gmail.com](mailto:revz.vijay@gmail.com))

Kalasalingam Academy of Research and Education Department of Physics <https://orcid.org/0000-0002-3288-9962>

**D Murugesan**

Bharathiar University

**Naidu Dhanpal Jayram**

Kalasalingam Academy of Research and Education Department of Physics

---

## Research Article

**Keywords:** metallic, Thermal evaporation, Dye detection and SERS

**Posted Date:** June 21st, 2021

**DOI:** <https://doi.org/10.21203/rs.3.rs-588087/v1>

**License:**  This work is licensed under a Creative Commons Attribution 4.0 International License.

[Read Full License](#)

---

# Abstract

Thin films and Surface Enhanced Raman spectroscopy have a strong bonding towards development of Sensors. From last 4 decades SERS has been used as effective tool for detection of toxic dyes, in food industry and agriculture world. To minimize the cost and fabrication over large surface is the most challenging task in substrate fabrication. In the present work an attempt has been made towards dual coatings, which could act as an effective SERS Substrates. An effective and facile approach of low cost bi-metallic Nanostructured film has been fabricated using thermal evaporation. Using the standard characterization techniques such as FE-SEM and XRD, the obtained films were Rhodamine 6G was used as an analyte for the SERS studies. The detection of R6G was up to  $10^{-10}$  mol  $l^{-1}$  solution. The present bi-metallic coating can be serves as an excellent SERS active surface and provides a versatile pathway to fabricate anisotropic nanostructure on a glass film.

## 1. Introduction

To overcome several limitations of Raman spectroscopy such as low cross section and scattering, and weak intensity over sensitive detection, Surface-enhanced Raman Scattering (SERS) technique came into being a most appropriate and broadly used spectroscopy technique for the analysis and identification of chemical and biological species (Juluri et al. 2015) in terms of both qualitative and quantitative analysis (Ignat et al. 2014; Yi et al 2012). Being surface sensitive, this mechanism is efficient in detecting the molecules at much lower concentration even at single-molecular levels (Wong-ek et al. 2010; Hu et al. 2016; Kneipp et al. 1997; Michaels et al. 1999; Xu et al. 1999). SERS is highly preferable and superior over the existing conventional detection techniques such as HPLC, GC-MS, ELISA. SERS enhancement basically involves two simultaneous mechanism such as electromagnetic enhancement (EM), referring to the excitation of localized surface plasmon resonance (LSPR) field by the collective oscillations of free electrons which is in the close vicinity of noble metallic nanostructures (Nie et al. 1997; Rajkumar et al. 2016; Nuntawong et al. 2013). In addition, small areas with profound intensified electromagnetic fields are generated known as hot spots (Zhang et al. 2013). In total, EM mechanism contributes to the major part of the enhancement factor ( $10^4$ – $10^7$ ). Chemical enhancement (CM), is refers to the charge transfer between the analytes molecules and the metallic nanostructures of substrates is known as another mechanism part of SERS (Wang et al. 2017). The order of enhancement factor by CM is usually  $10^1$ – $10^2$ . In order to get enhanced reproducibility with amplified enhancement factor, it is important to design proper nanostructures to maximize the LSP field coupling conditions which is the key research interest among the researchers from last few decades. To enhance SERS mechanisms, researchers have majorly employed noble metal nanoparticles like Gold (Au), Silver (Ag) and Copper (Cu) as a sensitizer compared to other materials (Yang et al. 2011; Yang et al. 2012; Chamuah et al. 2018) due to their surface plasmon resonance (SPR) (Jiao et al. 2019; Xie et al. 2018). Among all, Ag nanostructures have been widely used in SERS-active substrates for target analytes due to their good performance, broad plasmon resonance in the visible region, high surface reactivity, intensified signal enhancement and ease in preparation when compared to conventional metallic nanostructures. For SERS application, Ag nanostructures can be

fabricated into various shapes with different sizes such as nanoflowers, nanocubes, nanoplates, nanowires, nanochains etc. Due to these features, Ag nanoparticles serve as the potential and desirable nanostructure for SERS-active substrates (Shi et al. 2018). Currently, there is a growing interest in developing the bimetallic nanostructure on SERS substrates in order to enhance the functionality of monometallic nanostructures by introducing novel properties of the former (Jayram et al. 2015; Zheng et al. 2017). These bimetallic nanostructures are preferred due to their significant properties such as optical, electronic, catalytic, chemical, physical properties which are not found in aggregates or in bulk materials. Bringing two metallic nanoparticles together in single entity mainly alters the plasmonic nature of the two metals involved (Markin et al. 2018). Furthermore, their shape and size can be optimized and varied as per requirement. In particular, silver is a more efficient plasmonic material than gold and can be excited with more energetic light due to significantly reduced damping from interband transitions (Wang et al. 2016). Even though these colloids show high SERS enhancement factors, their stability always decreases (Hazra et al. 2017). In general both chemical and physical approaches are being used to produce the metal nanostructures for SERS application. In the chemical approach nanoparticles are prepared from the solution by reducing the metal salts. In these approaches the size and shape are controlled by controlling the experimental conditions of temperature, time, pH, concentration etc.(Jiang et al. 2018), and the use of surfactant plays a major role in controlling the size and shape. The surfactant and other stabilizing agents used during the preparation remain along with the nanoparticle, which cannot be completely get rid off. The synthesis of metallic nanoparticle by chemical method with reproducibility and stability is challenging. Nanoparticle dimerization, core-shell nanoparticle, three-dimensional hierarchical integration is some of the chemically synthesized nanostructures. Lithography is another ideal method for producing uniform and reproducible SERS substrates, but it is very expensive in a large-area production of the SERS substrates. Thin silver films (TSF) are widely used as SERS-active substrate also morphology of TSF surface determines its optical, Raman enhancing and adsorption properties as well as stability. In the present work an attempt has been made to fabricate and study bimetallic thin films, in which two kinds of metals are coined into one substrate. The substrate contains silver and copper dual coating and vice versa. This effective and facile approach has been named as fabrication of bi-metallic Nanostructured thin films using thermal evaporation. The Raman spectroscopic study shows that there is an enhancement in the Raman spectrum for the obtained bimetallic samples. Rhodamine 6G dye were used as analytes for the SERS studies.

## 2. Experimental

### 2.1. Preparation of bi-metallic thin films

Glass slides were cut in (1x1 cm) shape and surface contamination was removed by keeping the slides in aqua regia (HCl: HNO<sub>3</sub> = 3:1) for half an hour with further sonication in ethanol and final rinsing with distilled water. Prior to the preparation of bimetallic thin films, individual metal coatings were done using the different lengths of metal wires to obtain different thicknesses. Metal films having thicknesses of 30, and 50 nm (300 and 500 Å) were prepared by evaporating required metal from helical tungsten filament.

The thicknesses of the films were evaluated using an in-built quartz crystal thickness monitor. The bi-metallic Ag-Cu structure was prepared by coating 30 nm silver onto cleaned glass substrate and then coating 30 nm of copper over it. Similarly, Ag was coated over Cu for 30 and 50nm thickness. The deposition was done inside local made thermal evaporation system at working pressure of  $5 \times 10^{-6}$  pa. The deposition rate ( $3^\circ \text{As}^{-1}$ ) was measured using a quartz crystal monitor (QCM, Sigma Instruments, and SQM-160).

### 3. Results And Discussion

#### 3.1. Structural analysis of monometallic (Ag and Cu) and bimetallic (Ag-Cu and Cu-Ag) thin films

**Fig.1 (A)** shows the XRD pattern of silver thin films of two different lengths. The peaks at  $2\theta$  values of  $38.1^\circ$ ,  $44.09^\circ$  and  $77.29^\circ$  correspond to (111), (200), (311) planes of silver, respectively. Thus, the XRD spectrum confirmed the crystalline structure of silver films. No other peak corresponds to any impurity is seen. All the peaks in XRD pattern can be readily indexed to a face-centered cubic structure of silver as per available literature (JCPDS, File No. 4-0783). By using the Scherrer equation on the above peaks, the average size of the crystallites on the silver thin films is determined and tabulated in **Table.1**.

The lattice constant calculated from this pattern has been found to be  $a = 0.4085$  nm, which is consistent with the standard value  $a = 0.4086$  nm. **Fig.1 (B)** shows the XRD pattern of copper thin films of different thicknesses. The presence of peaks for 50 nm thick film at  $2\theta$  of  $43.25^\circ$ ,  $50.37^\circ$  and  $74.05^\circ$ , corresponds to (111), (200), (311) planes of copper, respectively. The 30 nm thick copper film exhibits amorphous nature. All the peaks in XRD pattern can be readily indexed to a face-centered cubic structure of copper as per available literature (JCPDS, File No.89-2838). By using the Scherrer equation on the above peaks, the average crystallite size in the copper thin films is determined and shown in Table 1. **Fig.1(C) and (D)** Shows the XRD patterns of Ag-Cu and Cu-Ag bimetallic thin films.

**Fig 1 (A) and (B)** shows the presence of silver and copper peaks at  $2\theta$  values  $38.1^\circ$ ,  $44.09^\circ$ ,  $77.29^\circ$ , corresponds to (111), (200), (311) planes of silver and copper respectively. The dominant peak of Ag (111) confirms the Ag prior to the copper. Similarly, in **Fig1 (C)** copper is having a dominant peak (111) at  $2\theta$  value of  $44.09^\circ$ . A low intensity silver peak at  $2\theta$  value  $38.1^\circ$  is also seen. The grain sizes were calculated using the Scherrer equation and tabulated in Table 2.

#### 3.2. FE-SEM Analyses of monometallic (Ag and Cu) and bimetallic (Ag-Cu and Cu-Ag) nanostructured thin films

**Fig.2** shows the FESEM images of silver and copper thin films of 30 and 50 nm thicknesses respectively prepared using thermal evaporation technique. The **fig 2. (a) and (b)** shows the morphology of randomly distributed silver nanoballs. Films with higher thickness show larger silver spheres in the size range of tens of nanometers. Similarly in copper films with smaller thickness, nanobeads with diameters of a few nanometers are seen (**Fig.2 (c)**). When the thickness is increased, not surprisingly, more of these small

copper beads developed into clusters. The copper clusters show highly dense beads with no gaps between two nanobeads.

The FE-SEM images in **Fig.2 (e)** shows that the Ag-Cu thin film has a highly aggregated nanobeads like structure and **Fig.2 (f)** the Cu-Ag thin film has aggregated nanoclusters like structure. Apart from this, no other clear or useful information is obtained from the FESEM analysis. FESEM images in **Fig.2 (e and f)** shows the aggregated nanobeads and nanoclusters like structures of Ag-Cu and Cu-Ag bimetals. In these bimetallic thin films, SERS intensity is found to be stronger for adsorbed molecules on the surfaces covered with aggregated nanoparticles. This shows the electric field is due to the aggregation in between the nanobeads and clusters results into higher order SERS (Yi et al. 2011). As seen in earlier sections, pure metallic thin films of copper and silver didn't show much high order enhancement for R6G  $10^{-10}$  and  $10^{-8}$  molar; but the bimetallic coating could able to detect dye concentration up to  $10^{-10}$  molar with clear spectrum. Hence it is evidenced that the aggregates structures gives room for the formation of more hot spots, that in turn help the detection of dye molecule even in their very low concentration level.

The Enhancement factor was also calculated according to the equation,

where  $I_{\text{surf}}$  and  $I_{\text{bulk}}$  are the integrated intensities of R6G molecules adsorbed on Ag-Cu nanocluster thin films for  $10^{-10}$  M and  $10^{-3}$  M of R6G bulk, respectively.  $N_{\text{surf}}$  and  $N_{\text{bulk}}$  are the corresponding numbers of R6G molecules adsorbed respectively on the SERS substrate and in the bulk solution effectively illuminated by the laser beam,  $N_{\text{bulk}} = AhC_{\text{bulk}}N_A$  where  $A$  is the area of the laser focal spot,  $h$  is the focal depth of the laser, and  $h$  is 13  $\mu\text{m}$ .  $C_{\text{bulk}}$  is the concentration of R6G bulk solution, here  $C_{\text{bulk}} = 10^{-3}$  M,  $N_A$  is the Avogadro constant for the below equation.

The above calculations were done using **Fig.6** for the 20  $\mu\text{l}$  R6G solution ( $1 \times 10^{-3}$  M) and the R6G - adsorbed on bimetallic thin films (Ag-Cu) ( $1 \times 10^{-10}$  M, 20  $\mu\text{l}$ ), which were spread on the  $1 \times 1 \text{ cm}^2$  prepared substrate. A laser spot area of 5  $\mu\text{m}$  and power of 15mW was applied with an accumulation number of 1sec for all recordings.

### 3.3 SERS Spectra for monometallic Ag and Cu and bimetallic Ag-Cu R6G and Cu-Ag R6G thin films

The particle size, shape and specific adsorption sites are the important factors in surface plasmon resonance (SPR). The junction between two Ag nano beads and Cu nano clusters acts as hotspot for the detection of low-density dye molecules. **Fig 3** shows SERS spectra of R6G dye with different concentrations ranging from  $10^{-5}$  to  $10^{-10}$  M adsorbed on Ag, Cu films. The Raman peaks are sharper for silver film with thickness 30 nm and show detection limit up to  $10^{-8}$  molar concentration. In case of 50 nm thick silver film, the R6G peaks are sharper but the detection limit is low compared to the other film. Due to the external electrical field applied on the nanobeads, they are polarized and consequently an enormous electrical field generate around it.

The electrical SPR is influenced by the thickness and roughness of the film or by random arrangement of the nanobeads. This effect results in higher order SERS intensity and hence the detection low of R6G dye molecule with concentration. Similar results are observed with copper films with thickness of 30 nm. Nanoscale structure and sharp points in metal nanostructures are the primary features needed to produce the highest possible enhancement in Raman scattering. Here individual Ag nanoballs structure with size of around 100 nm (**Fig.2**) which results in strong localized plasmon resonance and offers an opportunity to realize notable SERS enhancement in the case of silver thin films.

### 3.3.1. Influence of Ag and Cu film thickness on SERS response

The effect of the thickness of the silver and copper films on the SERS response was studied using the  $1365\text{ cm}^{-1}$  peak R6G dye of **Fig 3**. It is seen that the sensitivity of the silver substrate to adsorbed R6G dye is improved with higher thick metal film. Further increase of the film thickness (not shown in the figure) resulted in a decline in the sensitivity. When the thickness is increased from a minimal value, the number of larger silver clusters increased. Since these clusters are in the size range for optimal SERS enhancement, the response is improved. When the thickness is further increased, the clusters merged together which leads to the decrease in the SERS signal. Silver film with 50 nm thickness shows maximum response. In the case of copper, some SERS response is seen in film with 30 nm thick, whereas 50 nm and higher thickness films show very little SERS response.

From **Fig. 4**,  $I_{bulk}(1365\text{cm}^{-1})$  and  $I_{surf}(1361\text{ cm}^{-1})$  are determined as 24.10 and 48.10 cps respectively. Here the incident laser power is the same for normal Raman spectrum and SERS spectrum acquisition. Hence  $I_{surf} / I_{bulk}$  is calculated as  $48.10 / 24.10$ . The  $N_{bulk}/N_{surf}$  value is calculated to be  $32.656 \times 10^5$  and  $I_{SERS}/I_{bulk}$  is about 7.79 for the vibration peak at  $1367\text{ cm}^{-1}$ . Finally, the EF of this Ag-Cu SERS substrate is determined as  $6.5 \times 10^5$ .

## 5 Conclusion

It is evident that bi-metallic thin film coatings have good enhancement factor for both the Ag-Cu and Cu-Ag combinations. The obtained nanobeads like structure using Ag-Cu bimetallic thin film shows good response to the SERS. The present experiment clearly shows that the thickness and roughness of the film or the randomly arranged nanobeads alters the electrical SPR. Detection limit of bimetallic coating reaches upto  $10^{-10}$  molar with clear spectrum which are not shown by monometallic thin films. Hence it testifies that there is more formation of hotspots given by the aggregate's structures, helping in dye detection at very low concentration. The enhancement factor is low compared to metal oxide films, but still the current method provides a versatile and facile pathway to fabricate bimetallic strips for SERS analysis.

## Declarations

# Conflict of interest

On behalf of all authors, the corresponding author states that there is no conflict of interest.

# Acknowledgements

corresponding author N.D. Jayram wants to acknowledge SERB FILE NO.SRG/2019/001576 for providing start up research grant.

# References

1. Chamuah, N., Bhuyan, N., Das, P.P., Ojah, N., Choudhary, A.J., Medhi, T., Nath, P.: Gold-coated electrospun PVA nanofibers as SERS substrate for detection of pesticides. *Sens. Actuators B.* **273**, 710–717 (2018). doi:10.1016/j.snb.2018.06.079
2. Hazra, A., Hossain, S.M., Pramanick, A.K., Ray, M.: Gold-silver nanostructures: Plasmon-plasmon interaction. *Vacuum.* **146**, 437–443 (2017). <https://doi.org/10.1016/j.vacuum.2017.05.016>
3. Hu, C., Chen, S., Wang, Y., Liu, X., Liu, J., Zhang, W., ... Zhang, W.: Highly sensitive and well reproducible Surface-enhanced Raman spectroscopy from silver triangular platelets. *Talanta.* **161**, 599–605 (2016). <https://doi.org/10.1016/j.talanta.2016.08.008>
4. Ignat, T., Husanu, M.A., Munoz, R., Kusko, M., Danila, M., Teodorescu, C.M.: Gold nano-island arrays on silicon as SERS active substrate for organic molecule detection. *Thin solid films.* **550**, 354–360 (2014). <http://dx.doi.org/10.1016/j.tsf.2013.10.151>
5. Jayram, N.D., Sonia, S., Poongodi, S., Kumar, P.S., Masuda, Y., Mangalaraj, D., ... Viswanathan, C.: Superhydrophobic Ag decorated ZnO nanostructured thin film as effective surface enhanced Raman scattering substrates. *Appl. Surf. Sci.* **355**, 969–977 (2015). <https://doi.org/10.1016/j.apsusc.2015.06.191>
6. Jiang, D., Liang, H., Liu, Y., Zheng, Y., Li, C., Yang, W., ... Liu, J.: In situ generation of CoS 1.097 nanoparticles on S/N co-doped graphene/carbonized foam for mechanically tough and flexible all solid-state supercapacitors. *Journal of Materials Chemistry A.* **6**(25), 11966–11977 (2018). <https://doi.org/10.1039/C8TA04307H>
7. Jiao, A., Dong, X., Zhang, H., Xu, L., Tian, Y., Liu, X., Chen, M.: Construction of pure worm-like AuAg nanochains for ultrasensitive SERS detection of pesticide residues on apple surfaces. *Spectrochim. Acta Part A Mol. Biomol. Spectrosc.* **209**, 241–247 (2019). doi:10.1016/j.saa.2018.10.051
8. Juluri, R.R., Ghosh, A., Bhukta, A., Sathyavathi, R., Satyam, P.V.: Silver endotaxy in silicon under various ambient conditions and their use as surface enhanced Raman spectroscopy substrates. *Thin solid films.* **586**, 88–94 (2015). <https://doi.org/10.1016/j.tsf.2015.02.079>
9. Kneipp, K., Wang, Y., Kneipp, H., Perelman, L.T., Itzkan, I., Dasari, R.R., Feld, M. : S.:Single molecule detection using surface-enhanced Raman scattering (SERS). *Physical review letters.* **78**(9), 1667 (1997). <https://doi.org/10.1103/PhysRevLett.78.1667>

10. Markin, A.V., Markina, N.E., Popp, J., Cialla-May, D.: Copper nanostructures for chemical analysis using surface-enhanced Raman spectroscopy. *TrAC Trends Anal. Chem.* **108**, 247–259 (2018). <https://doi.org/10.1016/j.trac.2018.09.004>
11. Michaels, A.M., Nirmal, M., Brus, L.E.: Surface enhanced Raman spectroscopy of individual rhodamine 6G molecules on large Ag nanocrystals. *J. Am. Chem. Soc.* **121**(43), 9932–9939 (1999). <https://doi.org/10.1021/ja992128q>
12. Nie, S., Emory, S.R.: Probing single molecules and single nanoparticles by surface-enhanced Raman scattering. *science*, 275(5303), 1102–1106 (1997) <https://doi.org/10.1126/science.275.5303.1102>
13. Nuntawong, N., Eiamchai, P., Wong-ek, B., Horprathum, M., Limwichean, K., Patthanasettakul, V., Chindaudom, P.: Shelf time effect on SERS effectiveness of silver nanorod prepared by OAD technique. *Vacuum*. **88**, 23–27 (2013). <https://doi.org/10.1016/j.vacuum.2012.08.006>
14. Rajkumar, K., Jayram, N.D., Mangalaraj, D., Kumar, R.T.R.: One step ‘dip’ and ‘use’ Ag nanostructured thin films for ultrahigh sensitive SERS Detection. *Materials Science and Engineering: C*. **68**, 831–836 (2016). <https://doi.org/10.1016/j.msec.2016.07.032>
15. Shi, G., Wang, M., Zhu, Y., Wang, Y., Ma, W.: Synthesis of flexible and stable SERS substrate based on Au nanofilms/cicada wing array for rapid detection of pesticide residues. *Optics Communications*, 425, 49–57(2018) <https://doi.org/10.1016/j.optcom.2018.04.065>
16. Wang, X., Wang, R., Zhai, H., Shen, X., Wang, T., Shi, L., ... Sun, J.: Room-temperature surface modification of Cu nanowires and their applications in transparent electrodes, SERS-based sensors, and organic solar cells. *ACS Appl. Mater. Interfaces*. **8**(42), 28831–28837 (2016). <https://doi.org/10.1021/acsami.6b08984>
17. Wang, Z., Feng, L., Xiao, D., Li, N., Li, Y., Cao, D., ... Lu, N.: Silver nanoislands over silica spheres platform: enriching trace amount analytes for ultrasensitive and reproducible SERS detection. *Nanoscale*. **9**(43), 16749–16754 (2017). doi:10.1039/c7nr06987a
18. Wong-ek, K., Eiamchai, P., Horprathum, M., Patthanasettakul, V., Limnonthakul, P., Chindaudom, P., Nuntawong, N.: Silver nanoparticles deposited on anodic aluminum oxide template using magnetron sputtering for surface-enhanced Raman scattering substrate. *Thin Solid Films*. **518**(23), 7128–7132 (2010). doi:10.1016/j.tsf.2010.07.017
19. Xie, X., Pu, H., Sun, D.W.: Recent advances in nanofabrication techniques for SERS substrates and their applications in food safety analysis. *Critical reviews in food science and nutrition*. **58**(16), 2800–2813 (2018). doi:10.1080/10408398.2017.1341866
20. Xu, H., Bjerneld, E.J., Käll, M., Börjesson, L.: Spectroscopy of single hemoglobin molecules by surface enhanced Raman scattering. *Physical review letters*. **83**(21), 4357 (1999). <https://doi.org/10.1103/PhysRevLett.83.4357>
21. Yang, S., Lapsley, M.I., Cao, B., Zhao, C., Zhao, Y., Hao, Q., ... Huang, T.J.: Large-Scale Fabrication of Three-Dimensional Surface Patterns Using Template-Defined Electrochemical Deposition. *Adv. Func. Mater.* **23**(6), 720–730 (2012). doi:10.1002/adfm.201201466

22. Yang, S., Lei, Y.: Recent progress on surface pattern fabrications based on monolayer colloidal crystal templates and related applications. *Nanoscale*. **3**(7), 2768 (2011). doi:10.1039/c1nr10296f
23. Yi, Z., Chen, S., Chen, Y., Luo, J., Wu, W., Yi, Y., Tang, Y.: Preparation of dendritic Ag/Au bimetallic nanostructures and their application in surface-enhanced Raman scattering. *Thin solid films*. **520**, 2701–2707 (2012). <http://dx.doi.org/10.1016/j.tsf.2011.11.042>
24. Yi, Z., Xu, X., Li, X., Luo, J., Wu, W., Tang, Y., Yi, Y.: Facile preparation of Au/Ag bimetallic hollow nanospheres and its application in surface-enhanced Raman scattering. *Applied surface science*. **258**(1), 212–217 (2011). <https://doi.org/10.1016/j.apsusc.2011.08.033>
25. Zhang, W., Qiu, T., Qu, X.P., Chu, P.K.: Atomic layer deposition of platinum thin films on anodic aluminium oxide templates as surface-enhanced Raman scattering substrates. *Vacuum*. **89**, 257–260 (2013). <https://doi.org/10.1016/j.vacuum.2012.06.015>
26. Zheng, H., Ni, D., Yu, Z., Liang, P.: Preparation of SERS-active substrates based on graphene oxide/silver nanocomposites for rapid detection of L-Theanine. *Food Chem*. **217**, 511–516 (2017). <https://doi.org/10.1016/j.foodchem.2016.09.010>

## Tables

Due to technical limitations, table 1, 2, 3 is only available as a download in the Supplemental Files section.

## Figures

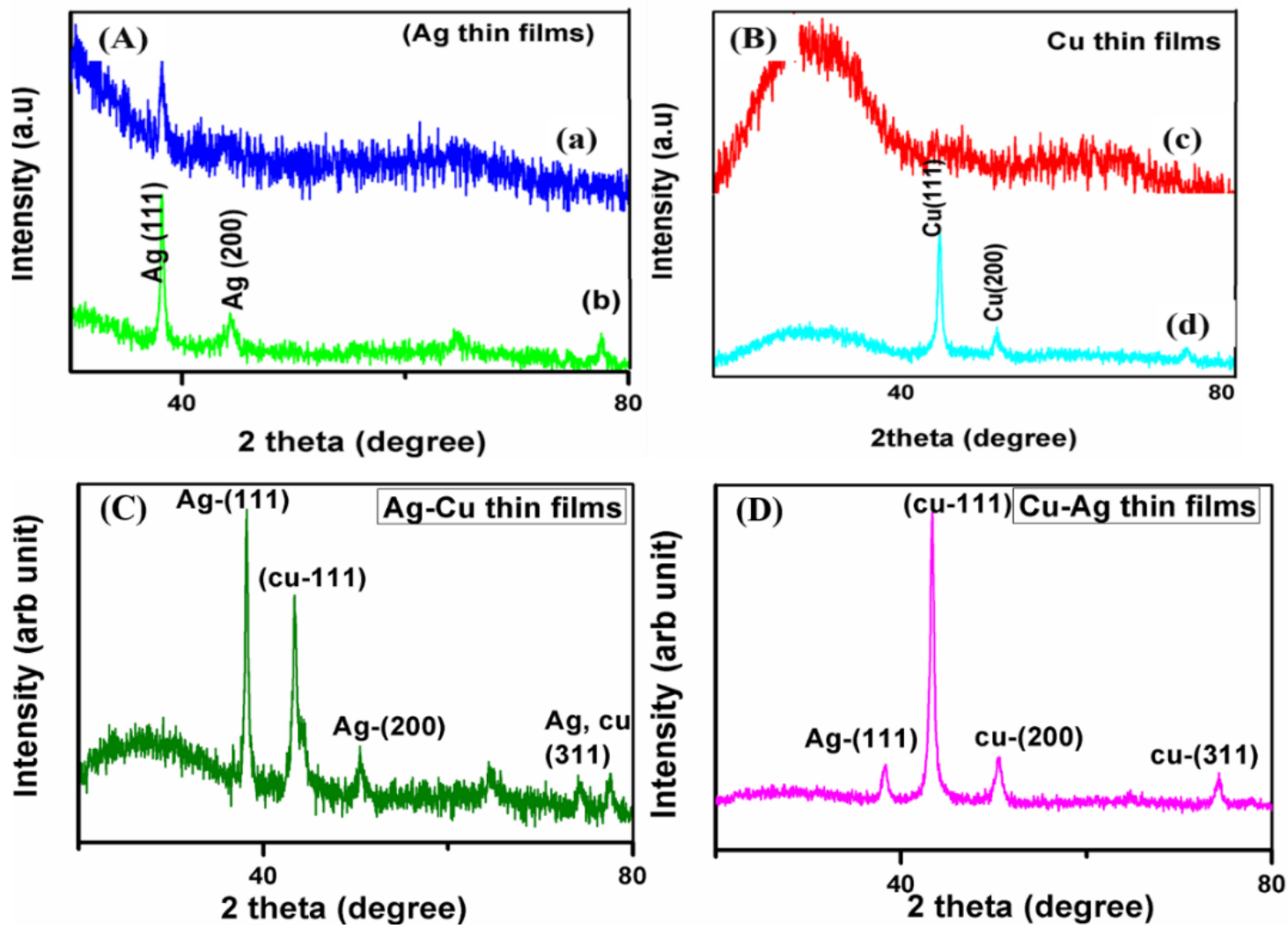
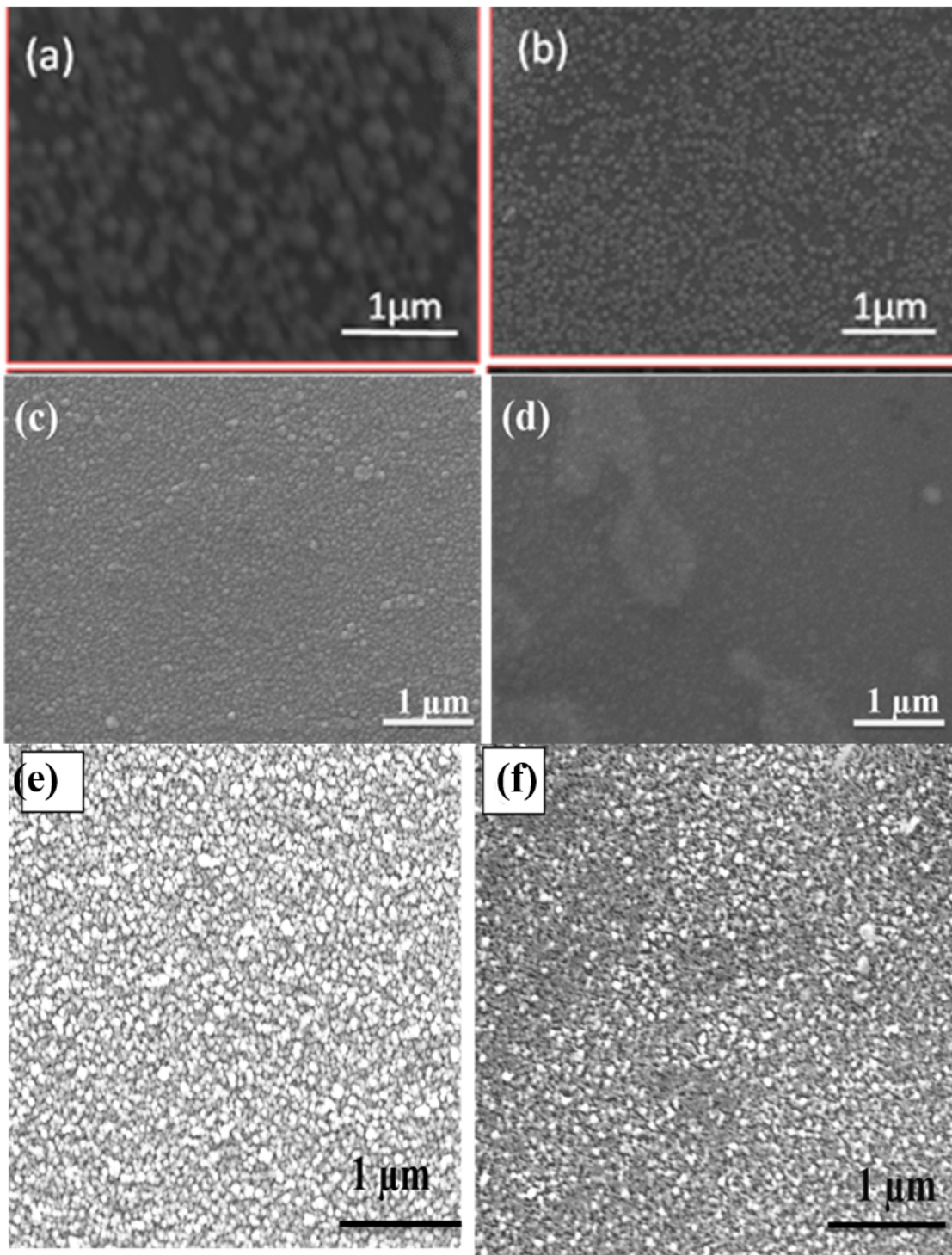


Figure 1

XRD analysis of (A) silver thin film for thickness (a) 30 and (b) 50 nm and (B) copper film for thickness (c) 30 and (d) 50 nm (C) silver-copper and (D) copper-silver bimetal structure with films thickness of 50 nm each.



**Figure 2**

Typical FESEM image of silver films of thicknesses (a) 30 (b) 50 nm and copper films with (c) 30 (d) 50 nm thickness (e) Ag/Cu and (f) Cu/Ag nanoclusters.

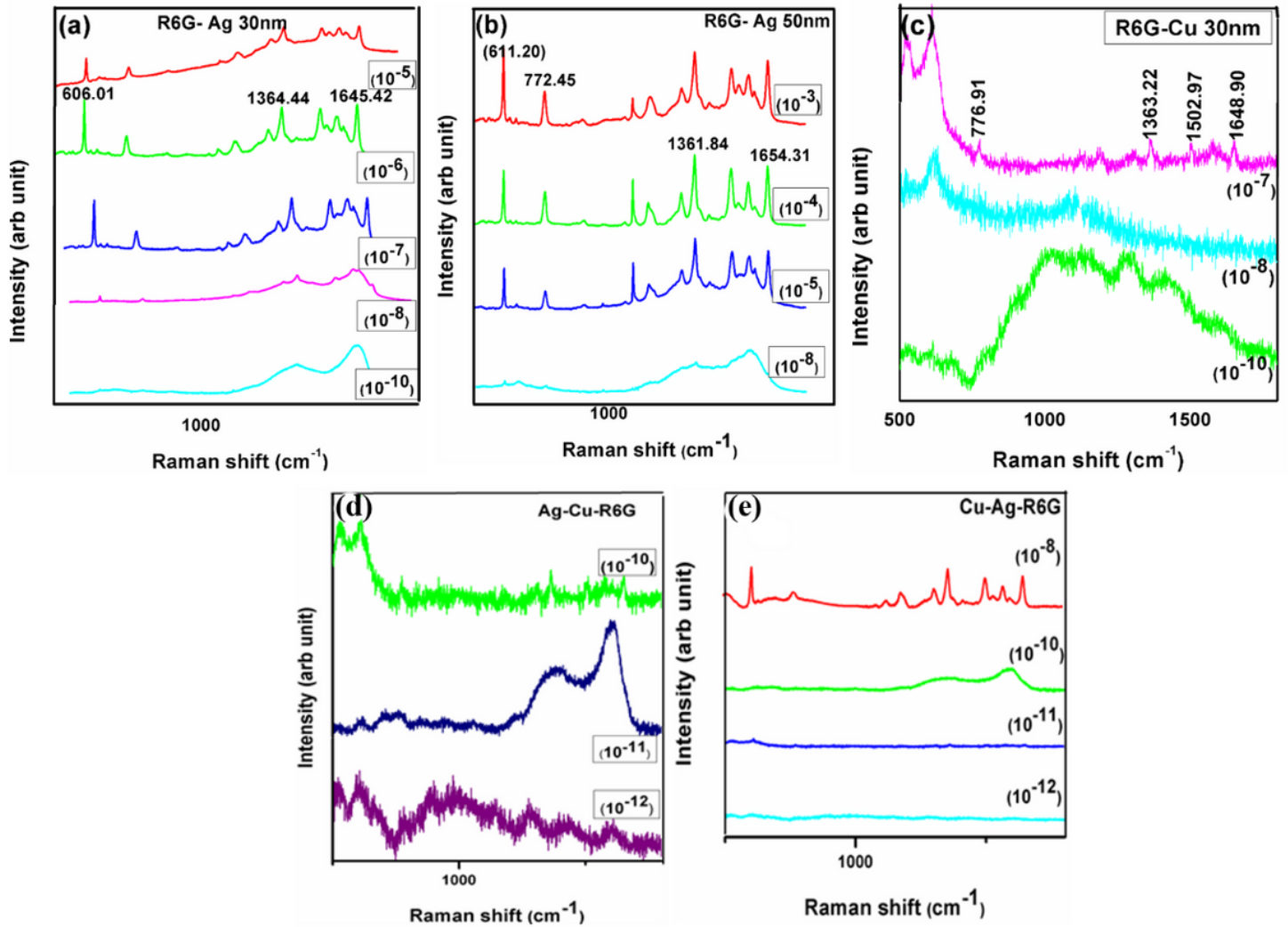


**Figure 3**

SERS spectra for Ag-R6G thin films (a) 30 (b) 50 nm (c) Cu-R6G 30 nm monometallic and (d) Ag-Cu R6G and (e) Cu-Ag R6G bimetallic thin films with different concentrations of R6G.

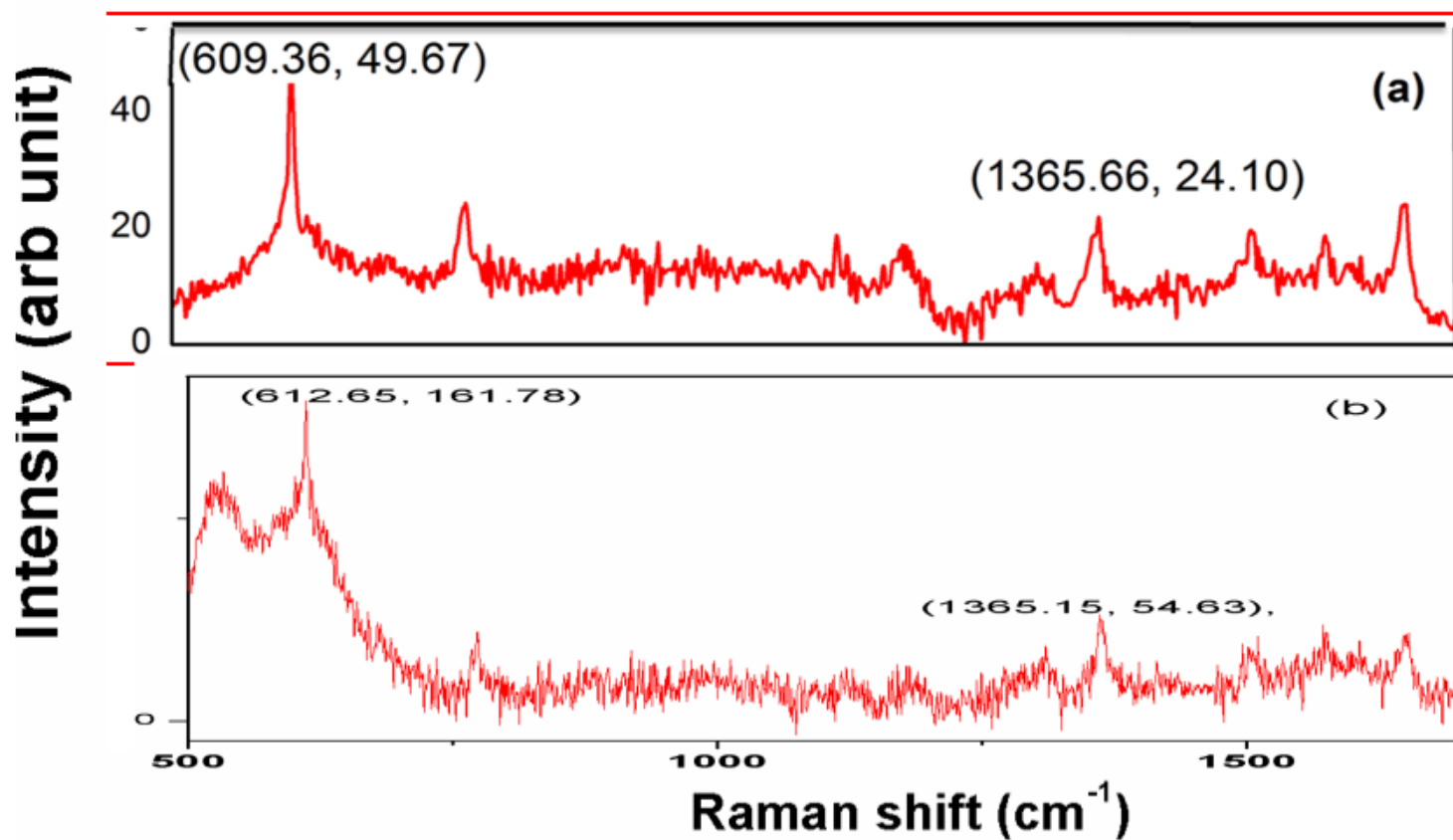


Figure 4

(a) Normal Raman spectra for R6G 10-3 and (b) SERS spectra of R6G using Ag-cu thin films for 10-11 molar dye.

## Supplementary Files

This is a list of supplementary files associated with this preprint. Click to download.

- [Tables.docx](#)